



<http://www.diva-portal.org>

Postprint

This is the accepted version of a paper presented at *IEEE International Electric Machines & Drives Conference (IEMDC) 2025, Houston, Texas, USA, May 18-21, 2025*.

Citation for the original published paper:

Ikram Ul Haq, O., Kanchan, R., Bosga, S., Peretti, L. (2025)
Multiphase Induction Machine Parameter Measurement Sensitivity Analysis
In: *IEEE International Electric Machines & Drives Conference (IEMDC), Houston, TX, USA, (2025)*

N.B. When citing this work, cite the original published paper.

Permanent link to this version:

<http://urn.kb.se/resolve?urn=urn:nbn:se:kth:diva-363303>

Sensitivity Analysis of Multiphase Induction Machine Parameter Identification Methods

Omer Ikram ul Haq
Dept. Energy Conversion
ABB Corporate Research Center
Västerås, Sweden
omer.ikramulhaq@se.abb.com

R. S. Kanchan
Dept. Energy Conversion
ABB Corporate Research Center
Västerås, Sweden
rahul.kanchan@se.abb.com

Sjoerd G. Bosga
Dept. Energy Conversion
ABB Corporate Research Center
Västerås, Sweden
sjoerd.bosga@se.abb.com

Luca Peretti
Div. of Electric Power and Energy Systems
KTH Royal Institute of Technology
Stockholm, Sweden
lucap@kth.se

I. ABSTRACT

Abstract—A multiphase induction machine (MPIM) modeled using vector space decomposition (VSD) provides insight into space harmonics which are segregated into vector spaces. Depending on the winding configuration of the MPIM, some vector spaces can produce torque in addition to the fundamental vector space, and they can be represented by a standard equivalent circuit (EC) of an induction machine (IM). This paper evaluates multiple EC parameters identification methods (IDMs) and proposes a robust IDM routine for their accurate estimation. Furthermore, the proposed IDM routine shows reduced sensitivity to errors in known parameters compared to the standard IDMs, which is validated with the help of a detailed simulation model of a 9-phase IM.

Index Terms—multiphase electric machines, induction motor, vector space decomposition, equivalent circuit, parameter identification methods

II. INTRODUCTION

Multiphase electrical machine (MPEM) with m phases provides m degrees of freedom, requiring suitable algebraic transformations to exploit their full potential in vector-control algorithms. Vector space decomposition (VSD) [1] is a possible transformation of choice for these types of machines. For a magnetically balanced machine, VSD decouple the space harmonics into $\lceil \frac{m}{2} \rceil$ vector spaces i.e $\nu \in \{1, 3, 5, \dots, \xi\}$ [2], where ξ is the largest odd number $\leq m$. These vector spaces are represented by independent equivalent circuits (ECs) having a unique set of parameters. Typically, the fundamental vector space, i.e., $\nu = 1$ is used for torque generation. However, $\nu \geq 3$ can be exploited to produce torque [3] which adds to the fundamental torque, enhancing the maximum torque capability of the machine. This feature of multiphase induction machines (MPIMs) is exploited in [4], where multiple vector spaces are excited simultaneously to produce the torque. For an accurate output torque production by each vector space ν , a precise set of EC parameters is required. In some cases,

these EC parameters are obtained using finite-element method (FEM) simulations. The precision of the parameters obtained through these methods is highly dependent on the details of the FEM model, manufacturing tolerances, and variations in material properties. Thus, field/laboratory measurements are preferred for robust parameter identification [5]. These methods provide accurate parameters for the fundamental vector space of MPIM. Nevertheless, these approaches have not been assessed for parameter identification in higher-order vector spaces. For the identification of higher-order vector spaces, the DC decay method [6] provides accurate parameters; however, it requires hardware modifications, making the identification procedure tedious. Depending upon the choice of EC parameter identification method (IDM), the accuracy of the estimated parameter is affected by the non-linearities of the converter voltage drop (CVD) as well as the accuracy of the known MPIM parameters.

This paper evaluates the sensitivity of multiple IDMs as a function of CVD and errors in the known parameters. These IDMs include DC injection test, no load test, locked rotor test, partial load test, and finally the constant rotor flux test. Descriptions of all these IDMs are discussed later under Section IV of this paper. Based on this sensitivity analysis, a parameter identification routine is devised which provides robust EC parameter identification. This devised routine is used in [7] for the measurement of the parameter of MPIM using the space harmonic relations.

III. MULTIPHASE INDUCTION MACHINE MODELLING

The MPIM model used in this paper is based on VSD [1], where the space harmonics are segregated into ξ vector spaces. The torque-producing property of a given vector space [2] depends on the choice of winding arrangement and its configuration [8]. The VSD transforms the space-vector quantities from the fundamental 123 reference frame (explained in [9]) to the stationary $\alpha\beta 0$ reference frame as given by (1). In this expression, $K = 1$ is used for amplitude-invariant transforma-

tions, whereas $K = 0.5$ for power-invariant transformations. δ is the angle between each magnetic phasor represented in half-wave symmetry [8].

$$\mathbf{x}_{\alpha\beta\gamma} = \underbrace{\left(\frac{2}{m}\right)^K \mathbf{C}_s}_{\mathbf{T}_{123 \rightarrow \alpha\beta\gamma}} \cdot \mathbf{x}_{123}; \quad \mathbf{x}_{123} = \underbrace{\left(\frac{2}{m}\right)^{1-K} \mathbf{C}_s^T}_{\mathbf{T}_{\alpha\beta\gamma \rightarrow 123}} \cdot \mathbf{x}_{\alpha\beta\gamma} \quad (1)$$

where:

$$\mathbf{C}_s = \begin{bmatrix} 1 & \cos(1\delta) & \cos(2\delta) & \dots & \cos((m-1)\delta) \\ 0 & \sin(1\delta) & \sin(2\delta) & \dots & \sin((m-1)\delta) \\ 1 & \cos(3\delta) & \cos(6\delta) & \dots & \cos((m-1)3\delta) \\ 0 & \sin(3\delta) & \sin(6\delta) & \dots & \sin((m-1)3\delta) \\ \vdots & \vdots & \vdots & \ddots & \vdots \\ 1 & \cos(\xi\delta) & \cos(2\xi\delta) & \dots & \cos((m-1)\xi\delta) \\ 0 & \sin(\xi\delta) & \sin(2\xi\delta) & \dots & \sin((m-1)\xi\delta) \end{bmatrix} \quad (2)$$

$$\delta = \frac{\pi}{m}; \quad \xi = \begin{cases} m & \text{if } m \text{ odd} \\ m-1 & \text{if } m \text{ even} \end{cases}$$

A generalized Park transformation brings the space-vector quantities from the $\alpha\beta\gamma$ reference frame to the rotating $dq0$ reference frame as expressed by (3), which is a block diagonal matrix with 2×2 blocks. A homopolar vector space is also available for certain types of winding configurations [2], which in this paper is set to 0. The remaining decomposed vector spaces ν can be expressed by independent ECs, as shown in Fig. 1, mathematically expressed by Eqs. (4) and (5). The parameters of each vector space are independent. This condition is met when the machine's stator or rotor iron core is not saturated.

$$\mathbf{T}_{\alpha\beta\gamma \rightarrow dq0} = \begin{bmatrix} a_{1,1} & \dots & a_{1,m} \\ \vdots & \ddots & \vdots \\ a_{m,1} & \dots & a_{m,m} \end{bmatrix}$$

$$\left\{ \begin{array}{l} a_{\nu,\nu} = a_{\nu+1,\nu+1} = \cos\left(\phi_{\omega_s}^{(\nu)}\right) \\ a_{\nu,\nu+1} = -a_{\nu+1,\nu} = \sin\left(\phi_{\omega_s}^{(\nu)}\right) \end{array} \right\} \quad \begin{array}{l} \text{for odd } \nu \\ \text{and } \nu \neq m \end{array} \quad (3)$$

$$\left\{ \begin{array}{l} a_{m,m} = 1 \\ 0 \end{array} \right\} \quad \begin{array}{l} \text{for odd } m \\ \text{otherwise} \end{array}$$

A. Equivalent circuit parameter

The topology of the EC chosen in this paper is the Γ -model shown in Fig. 1, defined by (4). This model is chosen specifically due to the ease of EC parameters identification and non-linear parameter modeling as explained in [10]. The accuracy of EC parameters defines the precision of field-oriented control (FOC) in the respective vector space. In most cases, an inv- Γ model is the EC of choice for torque-producing vector spaces. However, due to comparable magnitudes of magnetizing and leakage inductance of the higher-order vector spaces of a MPIM, identifying the EC parameters of the inv-

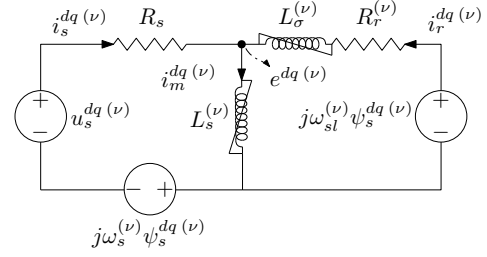


Figure 1: Γ dynamic model of MPIM in rotating reference frame representing vector space ν .

Table I: Γ model EC parameters of the 9-phase MPIM.

| ν | R_s [Ω] | $L_s^{(\nu)}$ [mH] | $L_\sigma^{(\nu)}$ [mH] | $R_r^{(\nu)}$ [Ω] |
|-------|-----------------------|-----------------------|----------------------------|-------------------------------|
| 1 | 0.37 | 155.9 | 7.5 | 0.2318 |
| 3 | 0.37 | 17.5 | 5.3 | 0.1978 |
| 5 | 0.37 | 5.1 | 4.3 | 0.1522 |
| 7 | 0.37 | 2.3 | 3.4 | 0.1281 |

Γ model is challenging. Furthermore, these inductances are highly non-linear and must be taken into consideration.

$$\begin{aligned} u_s^{dq}(\nu) &= i_s^{dq}(\nu) R_s + \frac{d}{dt} \psi_s^{dq}(\nu) + j\omega_s^{(\nu)} \psi_s^{dq}(\nu) \\ 0 &= i_r^{dq}(\nu) R_r^{(\nu)} + \frac{d}{dt} \psi_r^{dq}(\nu) + j\omega_{sl}^{(\nu)} \psi_r^{dq}(\nu) \end{aligned} \quad (4)$$

where

$$\begin{aligned} \psi_s^{dq}(\nu) &= L_s^{(\nu)} \left(i_s^{dq}(\nu) + i_r^{dq}(\nu) \right) \\ \psi_r^{dq}(\nu) &= L_s^{(\nu)} \left(i_s^{dq}(\nu) + i_r^{dq}(\nu) \right) + i_r^{dq}(\nu) L_\sigma^{(\nu)} \end{aligned} \quad (5)$$

and

$$\begin{aligned} \omega_{sl}^{(\nu)} &= \omega_s^{(\nu)} - \omega_r^{(\nu)} \\ S(\nu) &= \frac{\omega_s^{(\nu)} - \omega_r^{(\nu)}}{\omega_s^{(\nu)}} \end{aligned} \quad (6)$$

IV. DESCRIPTION OF IDMS

The Γ model EC parameters of the MPIM are divided into two categories, i.e., stator side parameters and rotor side parameters. The stator side parameter consists of stator resistance (i.e. R_s) and stator inductance (i.e. $L_s^{(\nu)}$), while the rotor side parameters are rotor resistance (i.e. $R_r^{(\nu)}$) and leakage inductance (i.e. $L_\sigma^{(\nu)}$). These parameters are identified using a sequence of IDMs which are given in Table II together with their corresponding number used in the control for the parameter identification routine. A generic control topology shown in Fig. 2, complemented by the current controller (CC) topology shown in Fig. 3, is used by each IDM. However, IDMs are only applicable to torque-producing vector spaces. In this paper, these IDMs are evaluated on a 9-phase symmetrical winding (SW) MPIM, which provides four torque-producing vector spaces and one homopolar component giving $\nu \in \{1, 3, 5, 7\}$ and $\gamma \in \{9\}$. The Γ model parameters of the 9-phase MPIM are given in Table I.

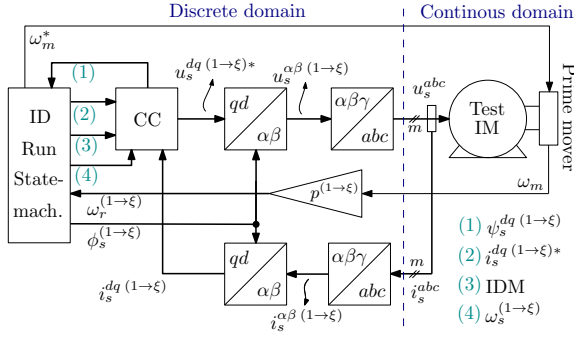


Figure 2: Simulated control topology for MPIM.

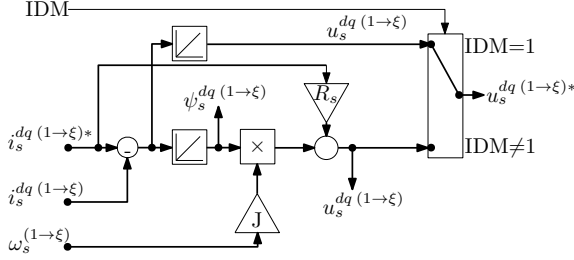


Figure 3: Simulated CC topology.

The sequence of IDMs is defined by "ID Run State Machine", which dictates the operating point of the system defined in Table III for each IDM. As the time constants of each EC are not known, the gains of the integrators and proportional-integral controller (PIC) are manually tuned to obtain a desired dynamic response. Furthermore, the proposed topology requires the test machine to be driven by a prime mover controlling the speed of the test MPIM. This allows measurements to be taken under no-load, locked rotor, and partial load conditions.

A. Stator side parameters

1) *DC injection test, IDM = 1*: DC injection is used for the identification of stator resistance R_s . During this test, $i_s^d(\nu)$, of the vector space ν is increased in steps until i_s^{\max} , which is usually defined by the current limit of the converter switches. At higher currents (preferably between 80% to 100% of i_s^{\max}), the CVD is expected to be linear. At these currents, the R_s is obtained by differential estimation and is given by (7), where Δu is the voltage component due to non-ideal inverter compensation (IC) (explained in [11]), which is approximately zero.

$$R_s = \frac{u_{s1}^d(\nu) - u_{s0}^d(\nu) + \overbrace{\Delta u}^{0 \text{ for large currents}}}{i_{s1}^d(\nu) - i_{s0}^d(\nu)} \quad (7)$$

where

$$\Delta u = \Delta u^d(i_{s1}^d(\nu)^*) - \Delta u^d(i_{s0}^d(\nu)^*) \quad (8)$$

A detailed simulation results of $IDM = 1$ is shown in Fig. 4 for a 9-phase MPIM. During this test, IC is not activated, showing the impact of CVD on the DC injection test. The

Table II: Description of IDMs and its corresponding number.

| IDM # | Method Name | Method Description |
|-------|--------------------------------|--|
| 1 | DC Injection | Identification of CVD and R_s . |
| 2 | No-load test | Identification of $L_s^{(\nu)}$. |
| 3 | Locked rotor test | Identification of $L_\sigma^{(\nu)}$ and $R_r^{(\nu)}$. |
| 4 | Constant $S^{(\nu)}$ test | Identification of $L_\sigma^{(\nu)}$ and $R_r^{(\nu)}$. |
| 5 | Constant $\psi_r^{(\nu)}$ test | Identification of $R_r^{(\nu)}$. |

Table III: IDM state-machine's reference table.

| IDM # | $i_s^d(\nu)$ | $i_s^q(\nu)$ | ω_m^* | ω_{sl} |
|-------|----------------------------|--------------|-------------------|-----------------------|
| 1 | $0 \rightarrow i_s^{\max}$ | 0 | 0 | 0 |
| 2 | $0 \rightarrow i_s^n(\nu)$ | 0 | $\omega_m^n(\nu)$ | 0 |
| 3 | $0 \rightarrow i_s^{\max}$ | 0 | 0 | $\omega_r^n(\nu)$ |
| 4 | $0 \rightarrow i_s^{\max}$ | 0 | $\omega_m^n(\nu)$ | $0.05\omega_r^n(\nu)$ |
| 5 | $0 \rightarrow i_s^{\max}$ | 0 | $\omega_m^n(\nu)$ | calculated |

impact of IC will be studied later in Section V of this paper. The selection of the vector space defines the practical phase order that constructs a given voltage vector as explained in [2] and does not affect R_s . Hence, R_s seen by each vector space is ideally the same.

2) *No-load test, IDM = 2*: During a no-load test, the motor is rotated at the synchronous speed (i.e. $\omega_s^{(\nu)}/p^{(\nu)}$) preferably with the assistance of a load machine. The load machine compensates for the friction and windage losses, reducing the $\omega_{sl}^{(\nu)}$ to zero, thus improving the accuracy of the measured $L_{ss}^{(\nu)}$, especially at low-currents. While the test MPIM is being rotated, the $i_s^d(\nu)^*$ is increased incrementally using the proposed control topology shown in Fig. 2. The resultant $u_s^{dq(\nu)}$ is recorded at steady-states at each current level. It is demonstrated in [12] that the stator voltage gets distorted and contains multiple harmonic components due to saturation. Due to this distortion $L_s^{(\nu)}$ obtained through simple steady-state impedance (i.e. $Z_0^{(\nu)}$) provides wrong estimation. However, the $u_s^{dq(\nu)}$ obtained through VSD of a MPIM filters out the voltage components of the non-active vector spaces, leading to a precise estimation of $L_s^{(\nu)}$ even when using a

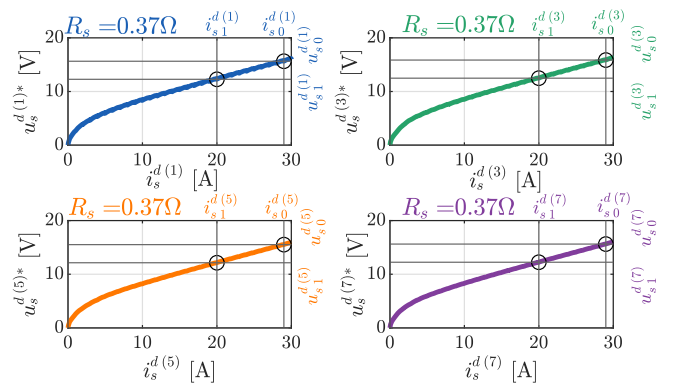


Figure 4: DC injection test showing results without IC.

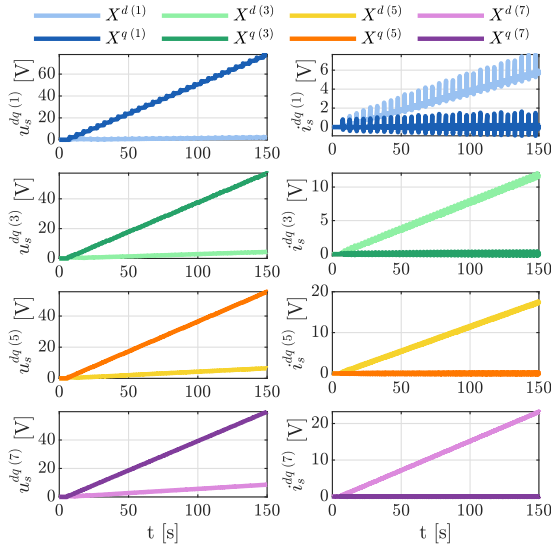


Figure 5: $u_s^{dq(\nu)}$ and $i_s^{dq(\nu)}$ of no-load test at $n_r = 700$ rpm.

basic $Z_0^{(\nu)}$ which is given by

$$Z_0^{(\nu)} = \frac{U_s^{(\nu)}}{I_s^{(\nu)}} \quad \text{and} \quad L_{ss}^{(\nu)} = \frac{\Im \left(Z_0^{(\nu)} \right)}{\omega_s^{(\nu)}} \quad (9)$$

The real component of stator impedance, i.e. $\Re(Z_0^{(\nu)})$, holds combined resistances of R_s , Iron losses, and skin-effect. Extraction of these parameters is challenging due to small magnitudes and hardware tolerances. However, in this paper, R_s obtained through the DC injection test is used as it reflects the actual stator resistance. A detailed simulation result of the no-load test is shown in Fig. 5 and the sensitivity of this IDM will be analyzed in Section V.

B. Rotor side parameters

In this paper, three different methods are evaluated for the identification of rotor side parameters i.e., locked-rotor test (i.e. IDM = 3), partial load test (i.e. IDM = 4), and constant $\psi_r^{(\nu)}$ (i.e. IDM = 5). The constant $\psi_r^{(\nu)}$ requires knowledge of $L_s^{(\nu)}$ and $L_\sigma^{(\nu)}$, which are obtained through IDM = 2 and 3 respectively. Thus, can be only used for the identification $R_r^{(\nu)}$. The $\psi_r^{(\nu)}$ controller manipulates $\omega_{sl}^{(\nu)*}$ to track $\psi_r^{(\nu)*}$. A control block diagram of $\psi_r^{(\nu)}$ controller is given in Fig. 6, where the $L_s^{(\nu)}$ and $L_\sigma^{(\nu)}$ are stored as a look-up table (LUT). Independent of the IDMs, the rotor side parameters are extracted from the rotor impedance, i.e. $Z_r^{(\nu)}$, which is given by Eq. (11). A detailed simulation result of each of the rotor side parameter IDMs is shown in Figs. 7 to 9 and the sensitivity of these IDMs will be analyzed in Section V.

$$R_r^{(\nu)} = \Re \left\{ Z_r^{(\nu)} \right\} S^{(\nu)}, \quad L_\sigma^{(\nu)} = \frac{\Im \left\{ Z_r^{(\nu)} \right\}}{\omega_s^{(\nu)}} \quad (10)$$

where:

$$Z_r^{(\nu)} = \frac{E^{(\nu)}}{I_m^{(\nu)} - I_s^{(\nu)}} \quad (11)$$

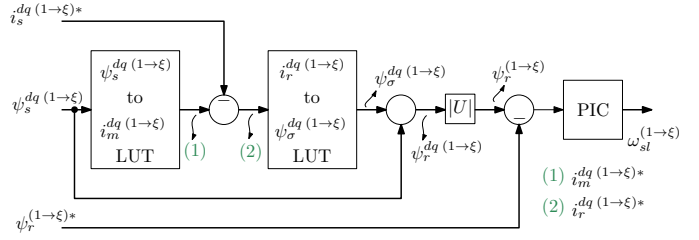


Figure 6: Generic $\psi_r^{(\nu)}$ controller topology.

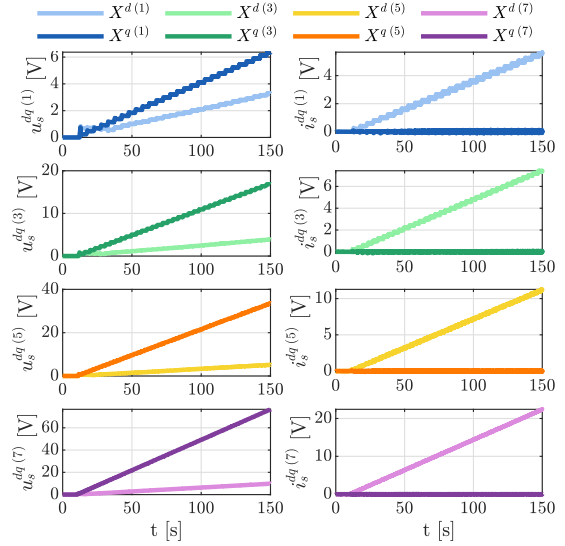


Figure 7: $u_s^{dq(\nu)}$ and $i_s^{dq(\nu)}$ of locked-rotor test.

and

$$I_m^{(\nu)} = \frac{U_s^{(\nu)} - R_s + I_s^{(\nu)}}{j\omega_s^{(\nu)} \bar{L}_m^{(\nu)}} \quad (12)$$

V. SENSITIVITY ANALYSIS

The connection between an IDM and the specific parameter it identifies is given in Table II. Each IDM e.g. IDM = x where $x \neq 1$, depends on the output of the preceding IDM i.e. IDM = $x - 1$. The IDM = $x - 1$ returns the parameters which are considered known parameters by IDM = x . The accuracy of IDM = x is evaluated against $\pm 20\%$ variation in the known parameters together with the impact of IC. During this sensitivity analysis, the DC link voltage and current measurements are assumed to be precise and do not influence the accuracy of the IDM. Furthermore, the sensitivity analysis is performed for all four torque producing vector spaces, i.e. $\nu \in \{1, 3, 5, 7\}$ of the 9-phase MPIM. The simulation results of each vector space are compiled in tabular form and given in Table IV, Table V, Table VI, and Table VII. These tables show the percentage error in the parameters estimated by each IDM. The "Ideal" column shows the error when the known parameters of the machine model and the IDM are initialized by the same value to establish a benchmark. The discrepancy in the "Ideal" column arises because the machine model operates in a continuous domain, whereas the IDM in

Table IV: IDM's sensitivity to known parameters for vector space 1. (Error given in %)

| Estimated Parameters | Ideal | CVD | | R_s | | $L_s^{(1)}$ | | $L_\sigma^{(1)}$ | | IDM description |
|----------------------|-------|--------|-------|-------|-------|-------------|--------|------------------|------|---|
| | | incl. | comp. | 80% | 120% | 80% | 120% | 80% | 120% | |
| R_s | -0,5 | 0,1 | X | X | X | X | X | X | X | DC injection test |
| R_s | -0,2 | 413,8 | X | X | X | X | X | X | X | No Load Test |
| $L_s^{(1)}$ | -0,5 | -0,4 | -0,4 | X | X | X | X | X | X | |
| $L_\sigma^{(1)}$ | 0,0 | -4,6 | 0,9 | -0,1 | 0,1 | 1,0 | -0,7 | X | X | Locked Rotor Test |
| $R_r^{(1)}$ | 0,0 | 505,9 | 2,1 | 34,9 | -35,1 | 2,0 | -1,4 | X | X | |
| $L_\sigma^{(1)}$ | 13,2 | -416,3 | 8,3 | -34,3 | 61,8 | -1554,0 | 1098,0 | X | X | Constant slip test $\omega_{sl}^{(1)} = 0.01\omega_r^{(1)}$ |
| $R_r^{(1)}$ | 0,4 | -5,4 | 0,5 | -0,2 | 1,0 | -13,5 | -8,5 | X | X | |
| $R_r^{(1)}$ | 0,0 | -5,1 | 0,9 | -0,6 | 0,7 | -0,3 | -2,3 | 0,1 | 1,0 | Constant $\psi_r^{(1)}$ test |

Table V: IDM's sensitivity to known parameters for vector space 3. (Error given in %)

| Estimated Parameters | Ideal | CVD | | R_s | | $L_s^{(3)}$ | | $L_\sigma^{(3)}$ | | IDM description |
|----------------------|-------|--------|-------|-------|-------|-------------|-------|------------------|------|---|
| | | incl. | comp. | 80% | 120% | 80% | 120% | 80% | 120% | |
| R_s | 0,0 | 0,6 | X | X | X | X | X | X | X | DC injection test |
| R_s | -0,3 | 279,4 | X | X | X | X | X | X | X | No Load Test |
| $L_s^{(3)}$ | -0,1 | 0,3 | 0,3 | X | X | X | X | X | X | |
| $L_\sigma^{(3)}$ | -0,1 | -7,7 | 0,5 | -0,3 | 0,0 | 7,2 | -4,4 | X | X | Locked Rotor Test |
| $R_r^{(3)}$ | -0,5 | 631,4 | 3,3 | 50,1 | -51,2 | 14,6 | -9,0 | X | X | |
| $L_\sigma^{(3)}$ | 9,4 | -218,5 | -1,7 | -51,9 | 84,8 | -973,7 | 771,9 | X | X | Constant Slip test $\omega_{sl}^{(3)} = 0.01\omega_r^{(3)}$ |
| $R_r^{(3)}$ | 0,0 | -24,1 | 0,1 | -6,2 | 7,0 | -56,4 | -42,5 | X | X | |
| $R_r^{(3)}$ | 0,0 | 3,8 | 0,3 | 0,3 | -0,2 | 4,3 | -8,8 | 0,0 | 0,0 | Constant $\psi_r^{(3)}$ test |

Table VI: IDM's sensitivity to known parameters for vector space 5. (Error given in %)

| Parameters | Ideal | CVD | | R_s | | $L_s^{(5)}$ | | $L_\sigma^{(5)}$ | | IDM description |
|------------------|-------|--------|-------|-------|-------|-------------|-------|------------------|------|---|
| | | incl. | comp. | 80% | 120% | 80% | 120% | 80% | 120% | |
| R_s | 0,0 | 0,6 | X | X | X | X | X | X | X | DC injection test |
| R_s | -0,3 | 215,8 | X | X | X | X | X | X | X | No Load Test |
| $L_s^{(5)}$ | -0,1 | 0,8 | 0,8 | X | X | X | X | X | X | |
| $L_\sigma^{(5)}$ | -0,3 | -11,0 | 0,5 | -0,6 | -0,2 | 23,6 | -11,7 | X | X | Locked Rotor Test |
| $R_r^{(5)}$ | -2,1 | 788,0 | 3,2 | 79,8 | -84,2 | 50,7 | -23,3 | X | X | |
| $L_\sigma^{(5)}$ | 13,7 | -143,2 | -5,2 | -61,8 | 153,1 | -541,9 | 418,8 | X | X | Constant slip test $\omega_{sl}^{(5)} = 0.01\omega_r^{(5)}$ |
| $R_r^{(5)}$ | 0,1 | -39,9 | 0,3 | -16,4 | 24,1 | -82,1 | -71,6 | X | X | |
| $R_r^{(5)}$ | -0,1 | 4,5 | 0,5 | 0,4 | 0,1 | 31,6 | -22,6 | -0,1 | -0,1 | Constant $\psi_r^{(5)}$ test |

Table VII: IDM's sensitivity to known parameters for vector space 7. (Error given in %)

| Parameters | Ideal | CVD | | R_s | | $L_s^{(7)}$ | | $L_\sigma^{(7)}$ | | IDM description |
|------------------|-------|--------|-------|-------|--------|-------------|-------|------------------|------|---|
| | | incl. | comp. | 80% | 120% | 80% | 120% | 80% | 120% | |
| R_s | -0,2 | 0,5 | X | X | X | X | X | X | X | DC injection test |
| R_s | -0,4 | 178,7 | X | X | X | X | X | X | X | No load test |
| $L_s^{(7)}$ | -0,2 | 0,8 | 0,7 | X | X | X | X | X | X | |
| $L_\sigma^{(7)}$ | -0,8 | -12,8 | -0,3 | -1,3 | -0,6 | 65,6 | -21,7 | X | X | Locked rotor test |
| $R_r^{(7)}$ | -6,5 | 602,3 | -3,2 | 95,2 | -109,0 | 161,5 | -41,9 | X | X | |
| $L_\sigma^{(7)}$ | 37,2 | -128,2 | 15,3 | -78,5 | 755,3 | -341,8 | 227,8 | X | X | Constant slip test $\omega_{sl}^{(7)} = 0.01\omega_r^{(7)}$ |
| $R_r^{(7)}$ | 0,0 | -56,2 | 0,2 | -34,4 | 104,6 | -95,7 | -91,7 | X | X | |
| $R_r^{(7)}$ | -0,3 | 10,4 | 0,2 | 3,0 | -0,5 | 97,9 | -40,0 | -0,3 | -0,3 | Constant $\psi_r^{(7)}$ test |

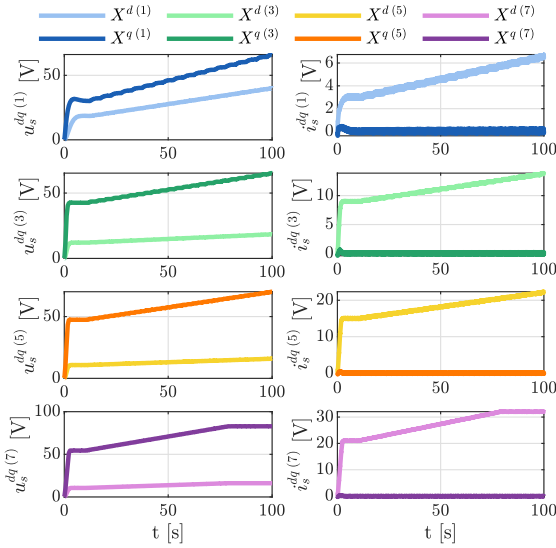


Figure 8: $u_s^{dq}(\nu)$ and $i_s^{dq}(\nu)$ of constant $\omega_{sl}^{(\nu)}$ test at $n_r = 700$ rpm, $\omega_{sl}^{(\nu)} = 0.01\nu\omega_m$ rad/s.

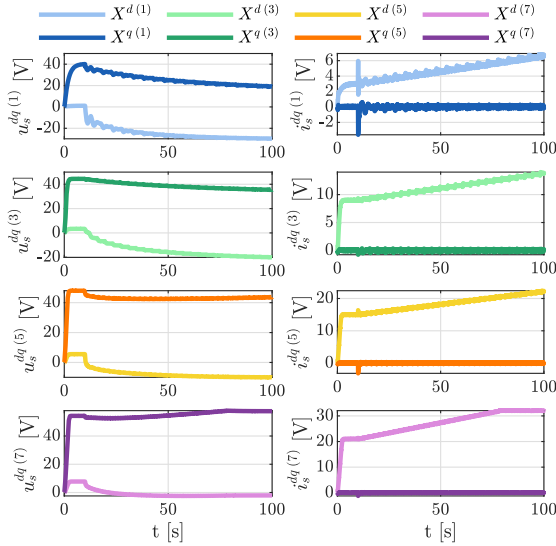


Figure 9: $u_s^{dq}(\nu)$ and $i_s^{dq}(\nu)$ of constant $\psi_r^{(\nu)}$ test at $n_r = 700$ rpm, $\psi_r^{(1)} = 0.5$ Vs, $\psi_r^{(3)} = 0.2$ Vs, $\psi_r^{(5)} = 0.12$ Vs, $\psi_r^{(7)} = 0.1$ Vs.

a discrete domain. The CVD column quantifies the impact of converter non-linearities and IC on the IDM, and finally, a 20% variation in the known parameters. The errors of $\geq 5\%$ in the estimated parameters are highlighted in red. This analysis shows that proper IC is important for accurate parameter identification except for the DC injection test. Additionally, precise estimation of $L_s^{(\nu)}$ is essential for accurate estimation of rotor side parameters, particularly in the context of higher-order vector spaces. The analysis also suggests that the locked rotor test provides a robust estimation of $L_\sigma^{(\nu)}$, while the constant $\psi_r^{(\nu)}$ test is used for the estimation of $R_r^{(\nu)}$ which provides robust results in comparison to the partial load and

locked rotor test. It is important to highlight that the $R_r^{(\nu)}$ of higher-order vector spaces is significantly affected by the skin-effect [7], which is not considered in this study.

VI. CONCLUSION

The paper evaluates multiple identification methods (IDMs) for the estimation of Γ equivalent circuit (EC) parameters of a 9-phase multiphase induction machine (MPIM). Based on sensitivity analysis, a robust parameter identification routine is devised, proposing an improved IDM i.e., constant $\psi_r^{(\nu)}$ test. The improved IDM is essential for an accurate estimation of the rotor resistance of higher-order vector spaces of a given MPIM. Furthermore, the parameter identification routine suggests the use of the DC injection test for the identification of stator resistance, the no-load test for stator inductance, the locked rotor test for compound leakage inductance, and finally a constant $\psi_r^{(\nu)}$ test for rotor resistance.

REFERENCES

- [1] A. A. Rockhill and T. A. Lipo, "A generalized transformation methodology for polyphase electric machines and networks," in *2015 IEEE International Electric Machines & Drives Conference (IEMDC)*. Coeur d'Alene, ID: IEEE, May 2015, pp. 27–34. [Online]. Available: <http://ieeexplore.ieee.org/document/7409032/>
- [2] O. Ikram ul Haq, L. Peretti, S. G. Bosga, and R. S. Kanchan, "Online Winding Reconfiguration of a Multiphase Stator," in *Power Electronics & Drive Systems (PEDS)*. Montreal, Canada: IEEE, Aug. 2023.
- [3] H. Liu, D. Wang, X. Yi, X. Zheng, and F. Cui, "Precise control of flat-topped air-gap magnetic field in a five-phase induction machine powered by third-harmonic-injected sinusoidal supply," *IEEE Transactions on Transportation Electrification*, pp. 1–1, 2022.
- [4] O. Ikram ul Haq, Y. Wu, L. Peretti, S. G. Bosga, and R. S. Kanchan, "Generalized harmonic injection strategy for multiphase induction machine control," *IEEE Transactions on Energy Conversion*, pp. 1–10, 2023.
- [5] H. S. Che, A. S. Abdel-Khalik, O. Dordevic, and E. Levi, "Parameter Estimation of Asymmetrical Six-Phase Induction Machines Using Modified Standard Tests," *IEEE Trans. Ind. Electron.*, vol. 64, no. 8, pp. 6075–6085, Aug. 2017. [Online]. Available: <https://ieeexplore.ieee.org/document/7870623/>
- [6] G. Falk Olson, Y. Wu, and L. Peretti, "Parameter estimation of multiphase machines applicable to variable phase-pole machines," *IEEE Transactions on Energy Conversion*.
- [7] O. Ikram Ul Haq, R. S. Kanchan, S. G. Bosga, and L. Peretti, "Equivalent circuit parameter measurement of multiphase induction machine by exploitation of space harmonic relations," *IEEE Access*, vol. 13, pp. 22 831–22 841, 2025.
- [8] M. Slunjski, O. Dordevic, M. Jones, and E. Levi, "Symmetrical/Asymmetrical Winding Reconfiguration in Multiphase Machines," *IEEE Access*, vol. 8, pp. 12 835–12 844, 2020. [Online]. Available: <https://ieeexplore.ieee.org/document/8955871/>
- [9] Y. Zhao and T. Lipo, "Modeling and control of a multi-phase induction machine with structural unbalance," *IEEE Trans. On energy Conversion*, vol. 11, no. 3, pp. 570–577, Sep. 1996. [Online]. Available: <http://ieeexplore.ieee.org/document/537009/>
- [10] E. Mölsä, L. Tiitinen, S. E. Saarakkala, L. Peretti, and M. Hinkkanen, "Standstill identification of an induction motor model including deep-bar and saturation characteristics," *IEEE Transactions on Industry Applications*, vol. 57, no. 5, pp. 4924–4932, 2021.
- [11] O. Ikram Ul Haq, R. S. Kanchan, C. Postiglione, S. G. Bosga, and L. Peretti, "Identification and compensation of converter non-linearities of a multiphase converter," in *2024 IEEE 33rd International Symposium on Industrial Electronics (ISIE)*, 2024, pp. 1–6.
- [12] L. Peretti and M. Zigliotto, "Automatic procedure for induction motor parameter estimation at standstill," *IET Electr. Power Appl.*, vol. 6, no. 4, p. 214, 2012. [Online]. Available: <https://digital-library.theiet.org/content/journals/10.1049/iet-epa.2010.0262>